

Single-molecule conductance oscillations in alkane rings.

Ali K. Ismael and Colin J. Lambert

Supplementary Information

Ali K. Ismael^{1,2}, Colin J. Lambert¹

¹Department of Physics, Lancaster University, Lancaster LA1 4YB, UK.

²Department of Physics, College of Education for Pure Science, Tikrit University, Tikrit, Iraq.

Correspondence: C.J.L. (email: c.lambert@lancaster.ac.uk), A.K.I. (email: k.ismael@durham.ac.uk)

Table of contents

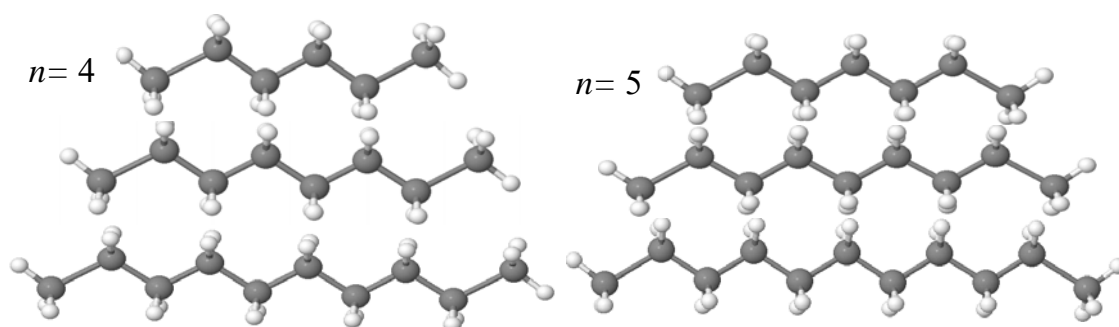
1. Geometry of isolated alkane linear and ring molecules	S1
2. Binding energy of three terminal groups on gold	S4
3. Binding energy of alkane ring and alkane linear chain on gold	S5
4. Conductance comparison between linear chains of different terminal groups	S6
5. Conductance comparison between linear chain and half ring	S7
6. Effect of confirmation on conductance	S8
7. A comparison between GGA and LDA	S11
8. Effect of changing bond distances and bond angles	S11
9. Quantum transport calculations	S12
10. A comparison alkane chains, rings and spiro-cycloalkanes	S13
11. References	S14

1. Geometry of isolated alkane linear and ring molecules

The DFT code (SIESTA)²⁸ was used to obtain fully relaxed geometries of the isolated alkane linear chains and rings, as shown in Supplementary Figure 1 and Supplementary Table 1 (including linear chains terminated with thiols and methyl sulphides). In this work, we choose three different alkane linear chains based on their terminal groups. The first chain is terminated with CH₃ groups, the second chain is terminated with SH groups and the last is terminated with SMe (methyl sulphides) groups (see Fig 1 in the manuscript). For alkane

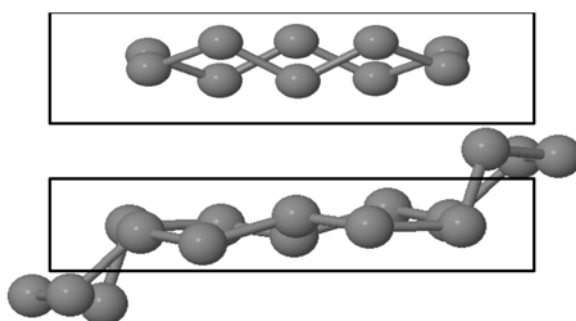
rings, we use just CH groups. We relax each ring starting from three different initial conformations to have accurate results. The length of each linear chain and ring varies from $n=4$ to 9 methylene ($n=CH_2$) units, as shown in Supplementary Table 1.

Here, we present the fully relaxed isolated conformations of six alkane linear chains. We started by four CH_2 units, then we increased the length by adding one unit each time until $n=9$. Increasing the length by one CH_2 unit switches the alkane chains from trans to cis (i.e. $n=4, 6$ and 8 chains are trans, while $n=5, 7$ and 9 chains are cis), as shown Supplementary Figure 1.



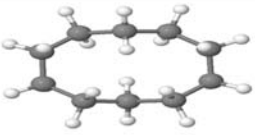
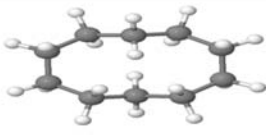

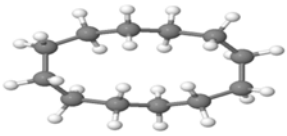
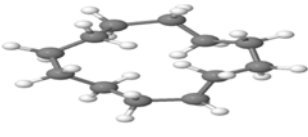
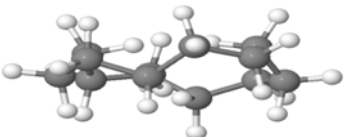
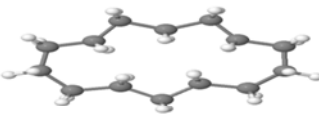
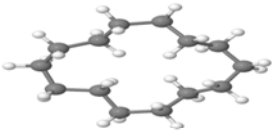
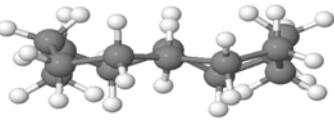
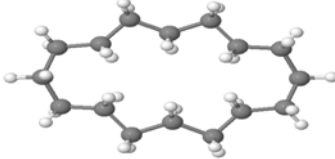
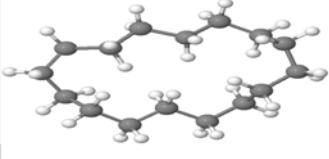
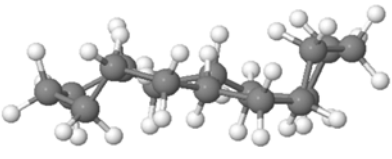
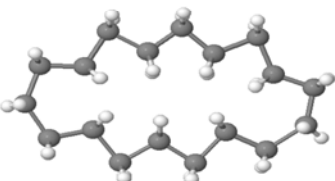
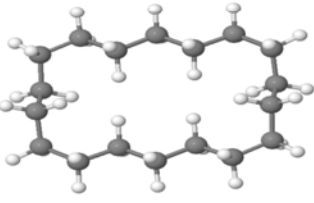
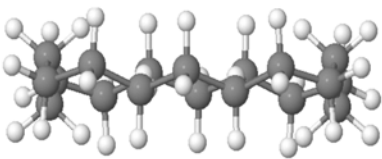
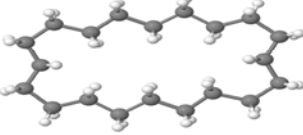
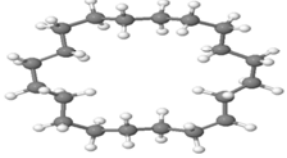
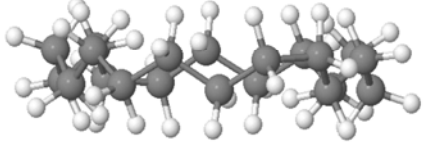
Supplementary Figure 1. Fully relaxed isolated molecules in two cases trans, length of 4, 6 and 8 CH_2 units (Left panel), and cis, with $n=5, 7$ and 9 CH_2 units (Right panel). Note that terminal groups are excluded from the definition of n .

For alkane ring relaxation, we start with the initial geometries shown in Supplementary Table 1 and obtain the fully relaxed geometries shown in Supplementary Table 1. The side views of the geometries reveal that the even-numbered rings tend to be more planar than the odd-numbered rings. As examples, Supplementary Figure 2 shows the relaxed geometries of $n=4$, and $n=7$ rings.



Supplementary Figure 2. Fully relaxed alkane rings of length of $n=4$ and $n=7$ CH_2 units. For clarity H atoms have been removed.

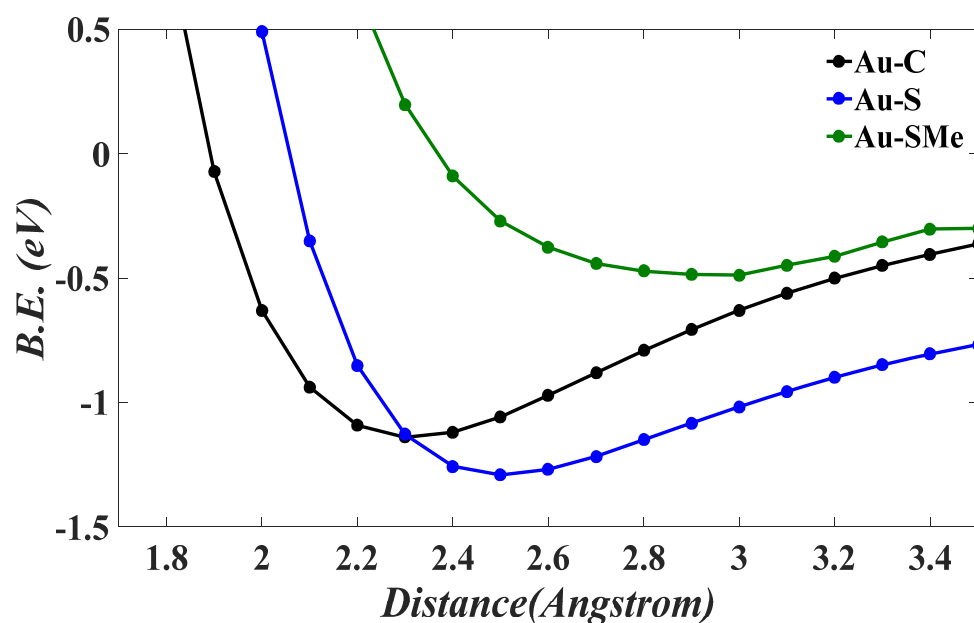
Supplementary Table 1. Initial start and fully relaxed geometries for isolated alkane ring cavities ($n=4, \dots, 9$ CH₂ units).

n	Initial geometry	Fully relaxed geometry	Side-view
4			
5			
6			
7			
8			
9			

2. Binding energy of three terminal groups on gold

To calculate the optimum binding distance for the alkane linear chains with different terminal groups (Au-C, Au-S and Au-SMe) binding to the gold (111) surfaces, DFT and the counterpoise method were used, which removes basis set superposition errors (BSSE). The binding distance was defined as the distance between the gold surface and the terminated end group/atom of the molecule. The ground state energy of the total system was calculated using SIESTA and is denoted E_{AB}^{AB} , with the parameters defined in the main text. Here the gold leads consist of 6 layers of 30 atoms. The energy of each monomer was then calculated in a fixed basis, which is achieved through the use of ghost atoms in SIESTA. Hence the energy of the individual molecule in the presence of the fixed basis is defined as E_A^{AB} and for the isolated gold as E_B^{AB} . The binding energy is then calculated using the following equation

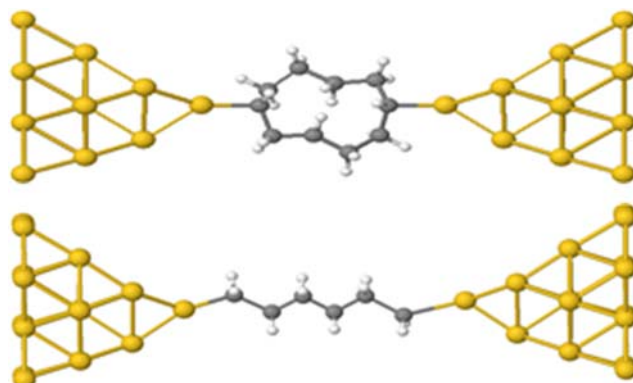
$$\text{Binding Energy} = E_{AB}^{AB} - E_A^{AB} - E_B^{AB} \quad (\text{S1})$$



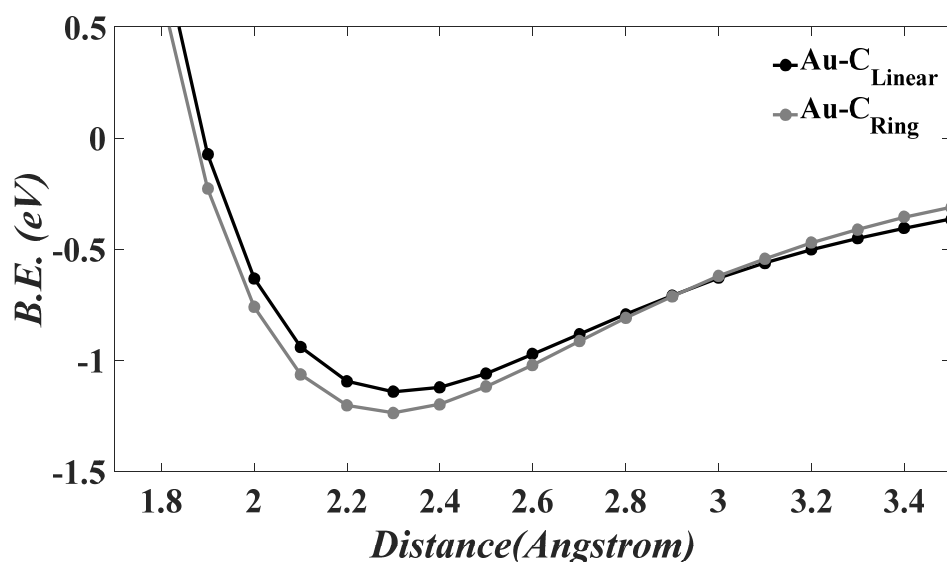
Supplementary Figure 3. Alkane linear chain derivatives on a gold tip: Binding energy of alkane linear chains to gold as a function of molecule-contact distance. The equilibrium distance (i.e. the minimum of the binding energy curve) is found to be approximately 2.3, 2.5 and 3.0 Å, for Au-C, Au-S, and Au-SMe (top to bottom).

3. Binding energies of alkane rings and alkane linear chains on gold

The next step is to compare the binding energies of alkane rings with their corresponding alkane linear chains (as shown in Supplementary Figure 4) in the presence of Au-C covalent bond, we repeat the same procedure that described above. Supplementary Figure 5 shows a comparison between the binding energy of an alkane ring and an alkane chain. Both curves have a strong binding to gold under-coordinated apex atom; the Au-C covalent binding energy is approximately 1.2 eV.



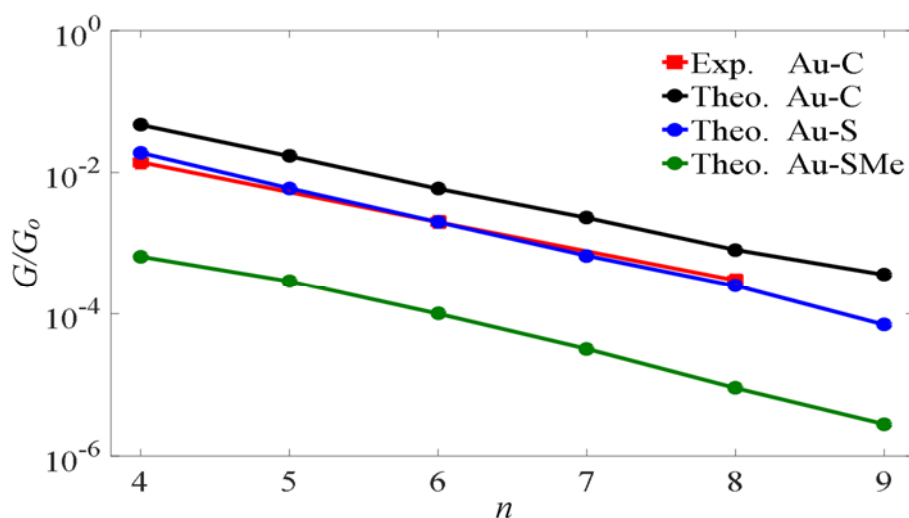
Supplementary Figure 4. Alkane ring and alkane linear chain in Au|molecule|Au junctions: the terminal group is Au-C ($n=4$ in both cases).



Supplementary Figure 5. The Au-C binding energy of $n=4$ alkane chain/ring to gold as a function of molecule-contact distance. The equilibrium Au-C distance (i.e. the minimum of the binding energy curve) is found to be approximately 2.3 Å, for both the chain and ring.

4. Conductance comparison between linear chains of different terminal groups

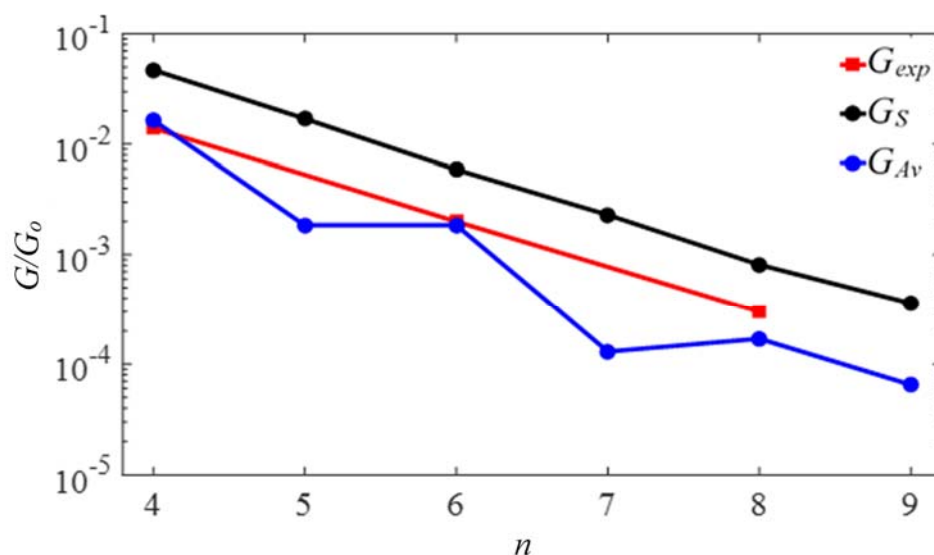
In this section, we compare the conductance G of linear chains of three different terminal groups, including covalent bond Au-C, thiols Au-S and methyl sulfides Au-SMe. Supplementary Figure 6 shows that the conductance G is highest for the covalent bond Au-C and lowest for the methyl sulphide (SMe) terminal group. These results in agreement with earlier experimental and theoretical studies.^{22-24,34-36} For comparison the red line in Supplementary Figure 6 shows experimental results ($n= 4, 6$ and 8)³⁷, for the conductances with Au-C bond at the electrodes. We make this comparison to benchmark our theoretical calculations against experimental measurements. The slope of this line is in good agreement with our theoretical results, although the intercept differs, partly because experimentally a range of unknown tip configurations are sampled.



Supplementary Figure 6. Chain-length dependence of the single-junction Au |alkane linear chain | Au conductance for three different terminal groups. DFT conductance as a function of length for three different terminal groups Au-C, Au-S and Au-SMe. A comparison between experiment³⁷, and theory for Au-C terminal group (red and black curves).

5. Comparison between the conductances of linear chains and frozen branches extracted from rings.

In this section, we compare the conductance G_s of a linear chain and the average conductance G_{Av} of frozen branches of the same length n . By comparing black and blue curves in Supplementary Figure 7, it is clear that G_s of alkane linear chains are larger than the average conductance G_{Av} of the upper and lower branches of the corresponding ring. We attribute this difference to their different relaxed geometries within the junction. For comparison, Supplementary Figure 7 also shows experimental results G_{exp} for the conductance of alkane chains with direct Au-C coupling.



Supplementary Figure 7. A comparison between the conductance G_s of linear chains (black circles) and the average conductance G_{Av} of frozen branches of the same length n (blue circles), obtained from DFT. For comparison, the red squares show the experimental results G_{exp} for linear chains reported in ref³⁷.

6. Effect of conformation on conductance

As it is mentioned above, $n=5$ and 7 rings have the less planar geometries than even-numbered rings. To examine the role of conformation on the conductance, we forced the odd cavities 5 and 7 into more planar conformations shapes (such as structure B in Supplementary Table 2). The black and red curves in Supplementary Figure 8 show the transmission functions of structures A and B respectively and demonstrate that forcing the chains into a more planar conformation increases their conductance.

Since for $n=5$, the energy difference between these conformations is only 0.034 eV, other conformations may be sampled in a real experiment. As examples, we created ten nearby conformations and calculated their total energies and transmission curves. The latter are also shown in Supplementary Figure 8 along with their ensemble averages (green lines) $\langle T(E) \rangle$ defined by

$$\langle T(E) \rangle = \sum_{i=1}^{10} T_i(E) \rho_i$$

where ρ_i is the Boltzmann factor

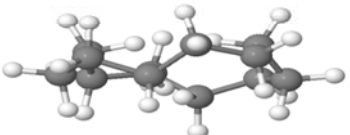
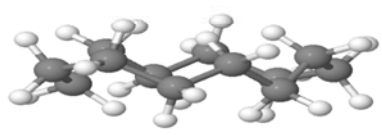
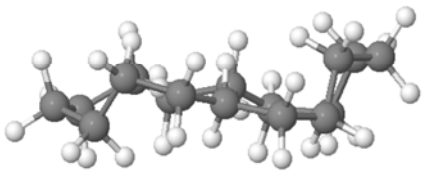
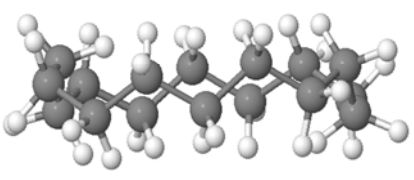
$$\rho_i = A e^{-\beta E_i}$$

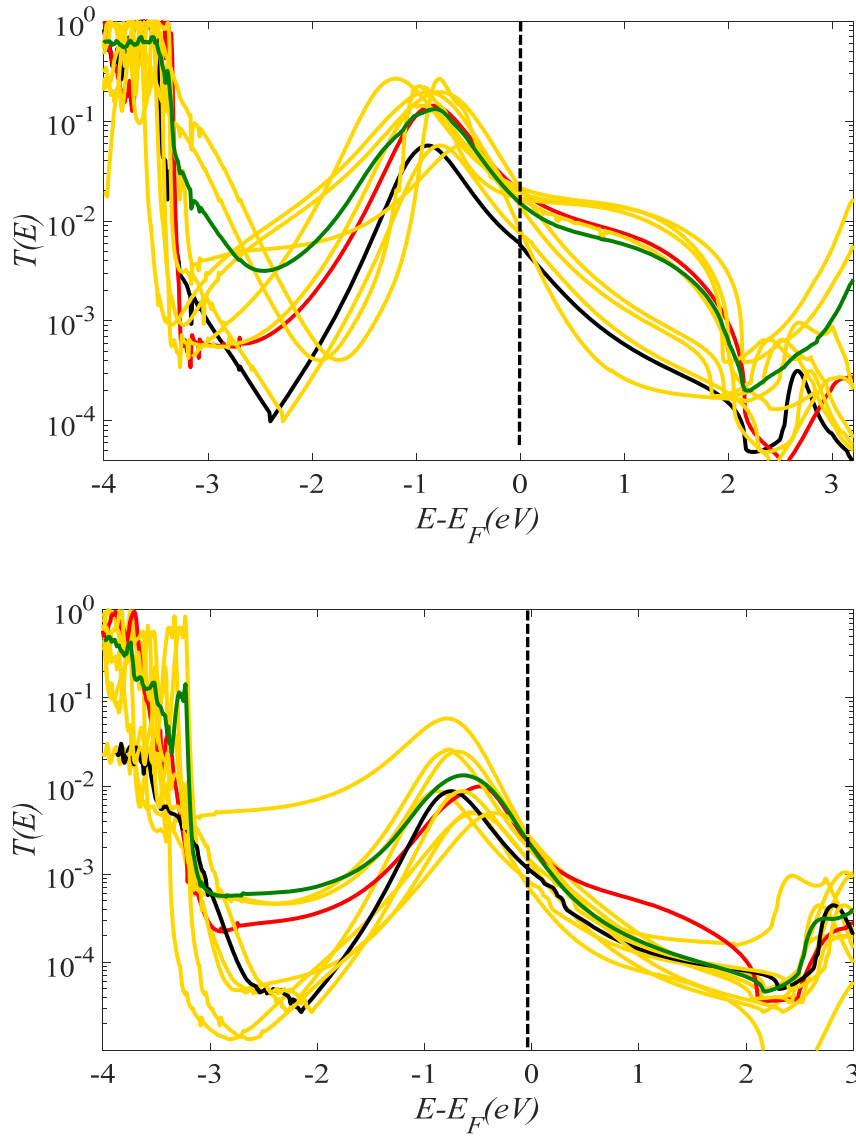
and

$$A = \sum_{i=1}^{10} e^{-\beta E_i}$$

These show that conductance oscillations may be removed by ensemble averaging at room temperature, in which case lower temperature measurements would be needed for their observation.

Supplementary Table 2. Non-planar geometry and more-planar geometries and their energy differences for odd cavities ($n= 5$ and 7 CH₂ units).

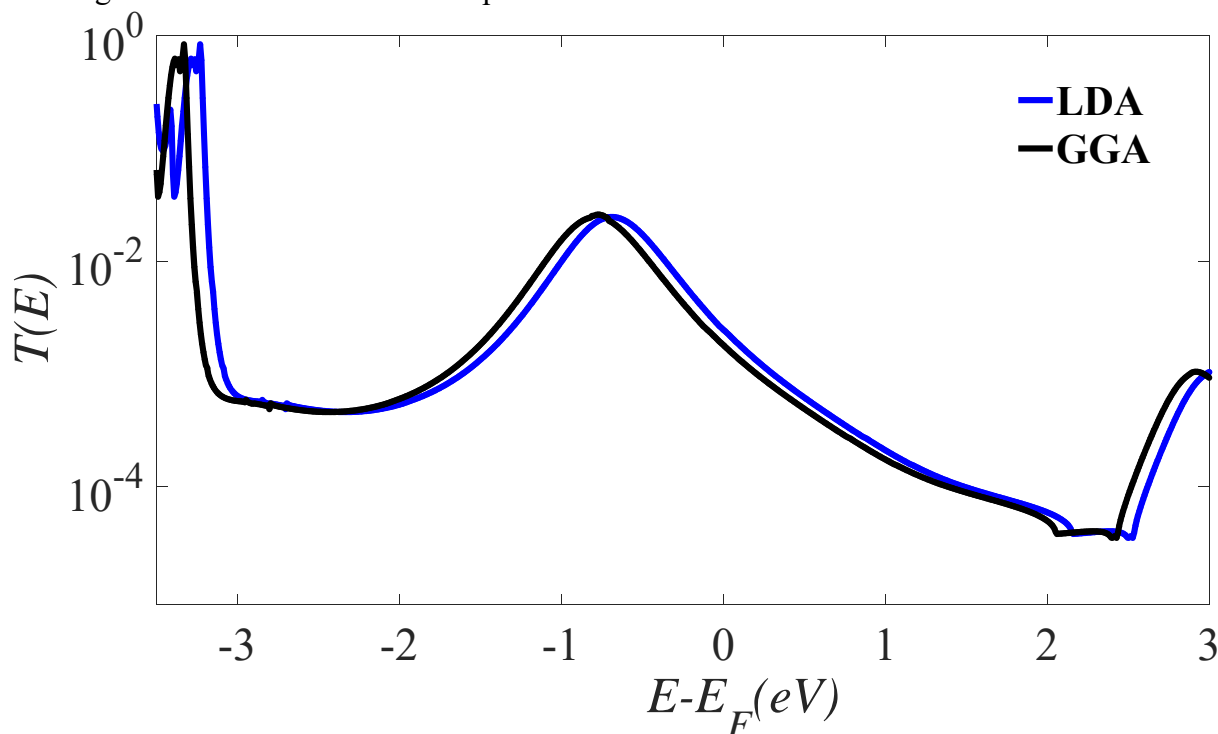
n	A. Fully relaxed geometry	B. Forced planar geometry	Energy difference ΔE (eV)
5			0.034
7			0.104



Supplementary Figure 8. The yellow curves show the transmission coefficients for a selection of the 10 possible configurations of $n=5$ (top panel) and $n=7$ (lower panel) rings. The green curves show the ensemble-averaged transmission $\langle T(E) \rangle$. Black and red curves correspond to structures A and B respectively..

7. A comparison between GGA and LDA

Herein, we compare two results by using LDA and GGA. Supplementary Figure shows the resulting transmission curves are comparable.



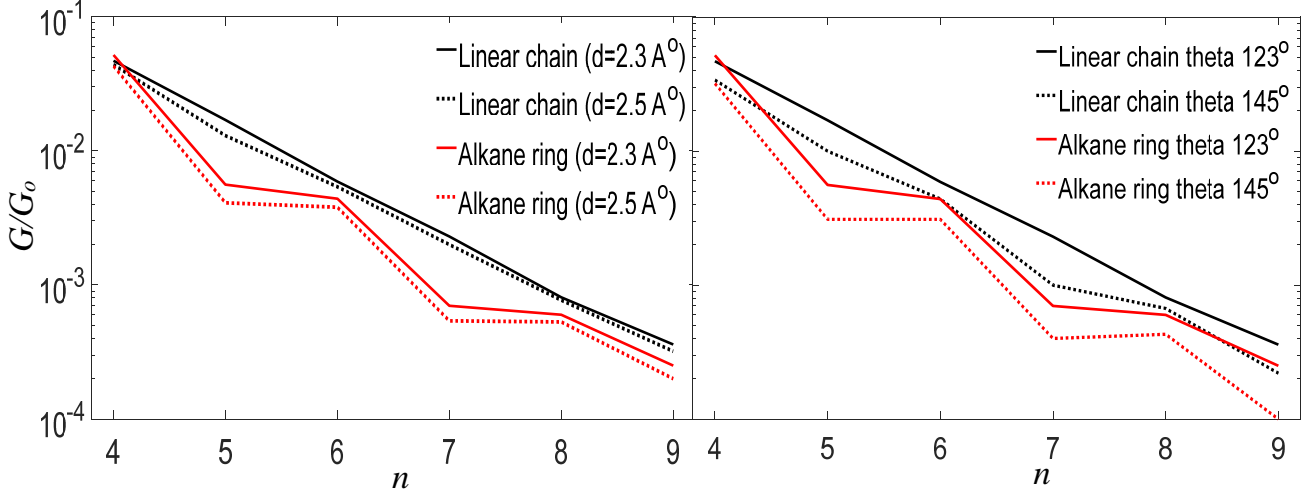
Supplementary Figure 9. Transmission coefficient curves for LDA and GGA, blue and black curve respectively.

8. Effect of changing bond distances and bond angles

As noted above, our calculations (see Supplementary Figure 3) find the most energetically favourable binding distance between the electrode and the end group. After determining the resulting relaxed geometries, they are kept the same for all calculations (For the terminal Au-C, the covalent bond distance is found to be 2.3 Å, with a Au-C-C angle of 123°. For the thiol terminal group, the Au-S distance is 2.5 Å, with a Au-S-C angle of 120° and for the SMe, the Au-S is slightly bigger at 3.0 Å, with a Au-S-C angle close to 180° as illustrated in Fig 1 in the manuscript (for more detail see Supplementary Figures 3 and 5).

Of course changing connection mode (by not taken the optimum values) will change the conductance. For example, increasing the covalent bond distance Au-C from the optimal value of 2.3 Å to 2.5 Å marginally lowers the conductance. Similarly, increasing or decreasing Au-C-C angle effects the conductance. However, the conductance ratios of linear chains versus alkane rings are approximately preserved and the same trends are obtained.

To illustrate this point, the Figure below shows the effect of changing the bond distance (left Figure) and bond angle (right Figure).



Supplementary Figure 10. Shows the effect of changing the connection mode. (Left panel) changing the distance between the electrode and the end group from 2.3 to 2.5 Å. (Right panel), changing the angle Au-C-C (θ) from 123 to 145°.

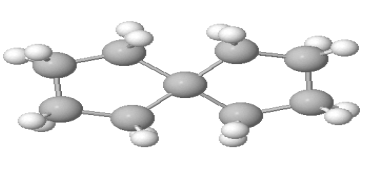

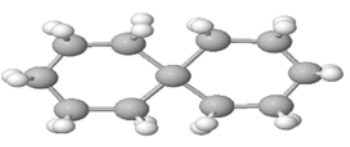
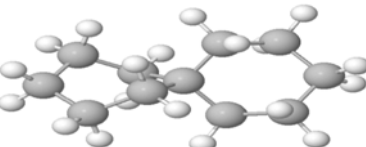
9. Quantum transport calculations

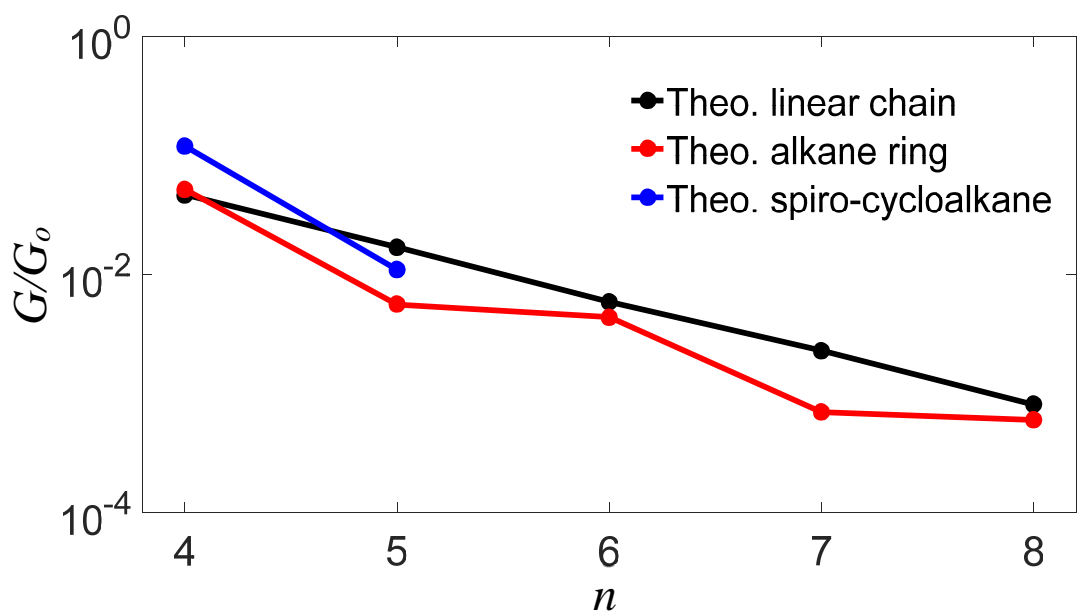
The mean-field Hamiltonian obtained from the converged DFT calculation was combined with our implementation of the non-equilibrium Green's function method, (the Gollum transport code,³³) to calculate the phase-coherent, elastic scattering properties of the each system consisting of left (source) and right (drain) leads and the molecule. The transmission coefficient $T(E)$ for electrons of energy E (passing from the source to the drain) is calculated via the relation: $T(E) = \text{Tr}(\Gamma_R(E)G^R(E)\Gamma_L(E)G^{R\dagger}(E))$. In this expression, $\Gamma_{L,R}(E) = i(\Sigma_{L,R}(E) - \Sigma_{L,R}^\dagger(E))$ describes the level broadening due to the coupling between left (L) and right (R) electrodes and the central scattering region, $\Sigma_{L,R}(E)$ are the retarded self-energies associated with this coupling and $G^R = (ES - H - \Sigma_L - \Sigma_R)^{-1}$ is the retarded Green's function, where H is the Hamiltonian and S is overlap matrix. From the transmission coefficient ($T(E)$), the room-temperature conductance is calculated via Landauer formula ($G = G_0 \int dE T(E)(-\partial f/\partial E)$) where $G_0 = 2e^2/h$ is the conductance quantum and $f(E) = (1 + \exp((E - E_F)/k_B T))^{-1}$ is the Fermi-Dirac distribution function, T is the temperature and $k_B = 8.6 \times 10^{-5}$ eV/K is the Boltzmann's constant.

10. A comparison between alkane chains, rings and spiro-cycloalkanes

As a comparison with the conductances of spiro-cycloalkanes, we have calculated the conductances of spiro[4.4]nonane and spiro[5.5]undecane, shown in Supplementary Table 3. As shown in supplementary Figure 11, their conductances are slightly higher than those of the corresponding alkane rings, follow the same trend of decreasing conductance with length.

Supplementary Table 3. Initial and fully relaxed geometries for isolated spiro-cycloalkanes ($n=4$ and 5 CH₂ units).

Spiro-cycloalkane	Initial geometry	Fully relaxed geometry
spiro[4.4]nonane		
spiro[5.5]undecane		



Supplementary Figure 11. A comparison between the conductance G of linear chains (black circles) and alkane rings (red circles) obtained from DFT, with Au-C bonds to the electrodes. For comparison, the blue circles show G for spiro-cycloalkanes.

11. References

1. M. J. Dewar, E. G. Zoebisch, E. F. Healy and J. J. Stewart, *Journal of the American Chemical Society*, 1985, 107, 3902-3909.
2. R. Pariser and R. G. Parr, *The Journal of Chemical Physics*, 1953, 21, 767-776.
3. J. J. Stewart, *Journal of computational chemistry*, 1989, 10, 221-264.
4. R. C. Bingham, M. J. Dewar and D. H. Lo, *Journal of the American Chemical Society*, 1975, 97, 1307-1311.
5. L. Buimaga-Iarinca and C. Morari, *The Journal of Physical Chemistry C*, 2013, 117, 20351-20360.
22. L. Venkataraman, J. E. Klare, I. W. Tam, C. Nuckolls, M. S. Hybertsen and M. L. Steigerwald, *Nano letters*, 2006, 6, 458-462.
23. B. Xu and N. J. Tao, *science*, 2003, 301, 1221-1223.
24. T. Lee, W. Wang, J. F. Klemic, J. J. Zhang, J. Su and M. A. Reed, *The Journal of Physical Chemistry B*, 2004, 108, 8742-8750.
28. M. Soler, E. Artacho, J. D. Gale, A. García, J. Junquera, P. Ordejón and D. Sánchez-Portal, *Journal of Physics: Condensed Matter*, 2002, 14, 2745.
33. J. Ferrer, C. J. Lambert, V. M. García-Suárez, D. Z. Manrique, D. Visontai, L. Oroszlany, R. Rodríguez-Ferradás, I. Grace, S. Bailey and K. Gillemot, *New Journal of Physics*, 2014, 16, 093029.
34. Y. S. Park, A. C. Whalley, M. Kamenetska, M. L. Steigerwald, M. S. Hybertsen, C. Nuckolls and L. Venkataraman, *Journal of the American Chemical Society*, 2007, 129, 15768-15769.
35. F. Chen, X. Li, J. Hihath, Z. Huang and N. Tao, *Journal of the American Chemical Society*, 2006, 128, 15874-15881.
36. D. Boese and H. Schoeller, *EPL (Europhysics Letters)*, 2001, 54, 668.
37. J. R. Widawsky, W. Chen, H. Vazquez, T. Kim, R. Breslow, M. S. Hybertsen and L. Venkataraman, *Nano letters*, 2013, 13, 2889-2894.